Presented at the
IAGA General Scientific Assembly,
Madrid, Spain, September 1-12, 1969

UCRL-19309
Preprint

cy. 2

RECEIVED
LAWRENCE
RADIATION LABORATORY
DEC 5 1969
LIBRARY AND
DOCUMENTS SECTION

LONG-TERM BEHAVIOR OF ENERGETIC INNER-BELT PROTONS

Harry H. Heckman, Peter J. Lindstrom,
and George H. Nakano

October 1969

AEC Contract No. W-7405-eng-48

TWO-WEEK LOAN COPY

This is a Library Circulating Copy which may be borrowed for two weeks. For a personal retention copy, call Tech. Info. Division, Ext. 5545

LAWRENCE RADIATION LABORATORY
UNIVERSITY of CALIFORNIA BERKELEY

UCRL-19309
cy. 2

DISCLAIMER

This document was prepared as an account of work sponsored by the United States Government. While this document is believed to contain correct information, neither the United States Government nor any agency thereof, nor the Regents of the University of California, nor any of their employees, makes any warranty, express or implied, or assumes any legal responsibility for the accuracy, completeness, or usefulness of any information, apparatus, product, or process disclosed, or represents that its use would not infringe privately owned rights. Reference herein to any specific commercial product, process, or service by its trade name, trademark, manufacturer, or otherwise, does not necessarily constitute or imply its endorsement, recommendation, or favoring by the United States Government or any agency thereof, or the Regents of the University of California. The views and opinions of authors expressed herein do not necessarily state or reflect those of the United States Government or any agency thereof or the Regents of the University of California.

LONG-TERM BEHAVIOR OF ENERGETIC INNER-BELT PROTONS

Harry H. Heckman
Lawrence Radiation Laboratory, University of California
Berkeley, California

Peter J. Lindstrom
Space Sciences Laboratory, University of California
Berkeley, California

and

George H. Nakano
Research Laboratories, Lockheed Missiles and Space Company
Palo Alto, California

October 1969

ABSTRACT

This report summarizes the experimental results on the temporal behavior, since late 1962, of low-altitude trapped protons, $E \geq 57$ MeV. These data are interpreted in terms of the time-dependent continuity equation, using a source function that is empirically deduced from the data. The observed changes in the flux of 63-MeV protons between 1963 and mid-1969 are in agreement with those expected from solar-cycle changes in the atmosphere. Preliminary calculations that include semiannual as well as solar-cycle atmospheric density variations indicate that, beginning in 1967, semiannual changes in the 60-MeV proton flux should be observable at altitudes below about 350 km. Our flux measurements are consistent with this computational result.

INTRODUCTION

Since late 1962, we have monitored the low-altitude trapped protons, $E \geqslant 57$ MeV, using emulsion detectors recovered from oriented, polar orbiting satellites. The nearly 7 years over which our observations have taken place constitute a significant part of the current 11-year solar cycle. As part of this work, properties of the inner-radiation-belt protons from September 1962 through June 1966, a period concurrent with solar minimum activity, have been examined in detail.[1] Throughout the solar minimum period the characteristic feature of the energetic trapped protons was its high degree of stability.

Coincident with increasing solar activity in mid-1966, we have had substantial evidence for a diminution in the proton flux at $E = 63$ MeV.[2] As of May 1969, the flux levels between 220 and 450 km altitude have decreased by more than a factor of two, relative to the solar minimum period. It appears that we are now very near the maximum of the present solar cycle. Consequently, the low-altitude proton flux is at, or near, its minimum value for this solar cycle.

In this paper we first report briefly on our latest results on the solar cycle variations in the proton flux, and review some of the pertinent features of the trapped protons during solar minimum that pertain to the altitude-flux profile and differential energy spectrum. The second part of this report presents some preliminary computational results, using the time-dependent continuity equation,[3-5] that are compared with experimental data.

PROPERTIES OF TRAPPED PROTONS 220 TO 450 km ALTITUDE

At low satellite altitudes, the inner radiation belt is detected only in the South Atlantic anomaly. This region, centered at approximately 34° S by 34° W, is the site of anomalously low intensities of the geomagnetic field, and hence, high fluxes of trapped radiation. Figure 1 shows the geometry of the South Atlantic anomaly. The solid-line contours are Injun 3 isoflux contours (in units cm^{-2} sec^{-1}) for protons in the energy interval $40 < E < 110$ MeV at an altitude of 400 km.[6] The contours of constant L, computed by using the 48-coefficient Jensen and Cain geomagnetic field model,[7] are shown as dashed lines. The northward trajectories traversing the anomaly region are those of a typical 4-day satellite flight at 400 km altitude and 75° orbit inclination. Demonstrated here is the uniform sampling of the particle fluxes in the anomaly, as well as the limited range of the L parameter. The magnetic field intensity, B, varies from 0.21 to 0.25 gauss over the range of L values shown.

The inner-belt protons exhibited a high degree of stability during the recent solar minimum period, September 1962 through June 1966;[1] in Figs. 2 through 5 we illustrate some of those temporally stable features of the inner-belt protons to which we refer in the second part of this report. Figure 2 presents the altitude dependence of the omnidirectional flux of E = 63 MeV protons. We plot in this figure the average daily flux, J (in units cm^{-2} MeV^{-1} day^{-1} and normalized to a 90° orbit inclination), observed for each satellite flight, versus the average minimum mirror-point altitude, $\overline{h}_{min}$. This flux refers only to those

protons detected during northward passes of the satellite in the anomaly (see Fig. 1). To remarkable precision, the altitude profile of the omnidirectional flux of 63-MeV protons can be fitted by a simple power-law function of the form $J(65\ \mathrm{MeV}) \propto \bar{h}_{min}^{n}$. The experimental data are shown as open circles and are fitted to a least-squares power law $J_c \propto \bar{h}_{min}^{4.67\pm0.08}$ to an accuracy of ±7.6% (SD). The computed daily fluxes for each flight, derived from the Injun 3 B-L proton flux contours and the satellite ephemerides, are shown as dark circles. The least-squares fit to these data yield an exponent $n = 4.05 \pm 0.04$. Although the differences between the slopes of the observed and computed altitude-flux profiles are statistically significant, we believe the Injun 3 data (recorded between December 24, 1962, and September 28, 1963) reproduce well our solar minimum data--clearly within the stated accuracy (20%) of the Injun 3 data.

Five measurements of the differential energy spectrum for protons, $E > 57$ MeV, between June 1963 and June 1966, are given in Fig. 3. The data are normalized to an altitude $\bar{h}_{min} = 375$ km, assuming the omnidirectional flux varies as $\bar{h}_{min}^{4.67}$, independent of energy. The errors of measurement are consistent with the spread in the data points. We have no evidence, therefore, for a change in the spectral shape of the protons during the solar minimum period. In fact, the energy spectrum obtained in 1960 by Heckman and Armstrong[8] (shown as a dashed line, and normalized at $E = 63$ MeV) also exhibits the same spectral shape. Thus, within the observational errors, the proton energy spectrum has been invariant for almost a complete solar cycle.

In what follows, we shall need to use the spectral shape of the spectrum between 50 and 90 MeV. For this energy interval, we take the spectrum to be $J(E) \propto E^{-0.72}$ cm^{-2} sec^{-1} MeV^{-1}. This energy spectrum was first derived by Freden and White,[9] and is in agreement with the observed spectrum for $50 < E < 90$ MeV.

Figure 4 presents the temporal behavior of the omnidirectional proton flux at 63 MeV between September 1962 and May 1969. Plotted as a function of time is the quantity $J(t)/J_c$, the ratio of the 63-MeV omnidirectional proton flux at time t to the least-squares flux observed during the solar minimum period (Fig. 2). The data are grouped into three altitude ranges: (a) $220 < \bar{h}_{min} < 300$ km, (b) $300 < \bar{h}_{min} < 400$ km, and (c) $400 < \bar{h}_{min} < 455$ km. Within the experimental errors (the 5% statistical errors are indicated for the 300–400-km interval) we conclude that <u>the flux of 63-MeV protons was, for all practical purposes, in a steady state at all altitudes between 220 and 455 km during the period November 1962 to June 1966.</u>

Variations in the proton flux before and after the quiescent period are readily apparent. The high value of the flux observed in September 1962, our first measurement, can be attributed to the effects of the Starfish nuclear detonation in July 1962 on the inner-belt protons.[10] Near mid-1966, the proton flux began to decline, and, as of May 1969, had decreased to about 0.40 of its solar minimum value.

CONTINUITY EQUATION: COMPUTATIONS

Solar Cycle Variations

It is these experimental results that we wish to discuss in terms

of the time-dependent continuity equation,[4, 9]

$$\frac{dN}{dt} = S - \frac{d}{dE}\left(v\, N(E)\, \frac{dE}{dx}\right) - \rho\sigma v N, \qquad (1)$$

where N = particle density in units $cm^{-3}\ MeV^{-1}$,

and S = source strength in $cm^{-3}\ sec^{-1}\ MeV^{-1}$.

The second and third terms on the right are, respectively, the rates of particle loss owing to energy loss by ionization and nuclear interactions in the residual atmosphere. For the atmospheric density averaged over the particles' trajectory, ρ, we shall use the results of Heckman and Brady.[11] In our present calculations, the results of Heckman and Brady, which are based on the Harris and Priester model atmosphere, are reformulated in terms of $F_{10.7}$ (in units of 10^{-22} W M^{-2} cps^{-1}), the 10.7 solar flux.[12, 13] Furthermore, we have augmented the atmospheric density calculation to permit the evaluation of the effective atmospheric densities as a function of $F_{10.7}$ as well as E, the proton energy. The latter correction enters because the atmosphere traversed by a trapped particle is dependent on its cyclotron radius, hence energy, for a given minimum mirror-point altitude of the particle's guiding center.[11]

The experimental data cited above, when incorporated into solutions of Eq. 1, should give us some insight as to the source strength, its altitude dependence, and the temporal behavior of the trapped protons. Explicitly, the data state that, in the energy interval $50 < E < 90$ MeV,

(a) $dN/dt \approx 0$ between 1963.0 and 1966.0,

(b) $N(h_{min}) \propto h_{min}^{4.67}$, $250 < h_{min} < 450$ km, and

(c) $N(E) \propto E^{-0.72}$.

Given the time-dependent effective atmospheric density, $\rho[h_{min}, E, F_{10.7}(t)]$, where $F_{10.7}(t)$ is the monthly averaged 10.7-cm solar flux, our objective is to solve for the energy and altitude dependence of the source function, $S(E, h)$, from which the particle density $N(E)$ can be computed as a function of time and altitude.

To prepare Eq. (1) for integration, we follow Freden and White[9] and express the velocity, v, and rate of energy loss, dE/dx, in terms of power-law relationships in energy, E, for the interval $50 < E < 90$ MeV. Given a source strength, S, and a proton density at time t, $N(E, t)$, then, at time $t + \Delta t$,

$$N(E, t+\Delta t) = N(E, t) + \frac{dN(E, t)}{dt} \Delta t. \qquad (2)$$

Integration errors in Eq. 2 are less than 0.1% for step size $\Delta t = 1$ to 2 hours.

The first question we ask is: Is there an $S(E, h)$ such that an approximate steady-state solution is given by Eq. 1 between 1963.0 and 1966.0, independent of E and h? The answer is Yes. As a particular example, Fig. 5 gives $S(h)_{obs}$ for 60-MeV protons that yields flux values that are practically constant during the solar minimum period, $250 \lesssim h_{min} \lesssim 450$ km. The errors assigned to $S(h)_{obs}$ represent the uncertainty in the source function that arise from the approximately ±10% scatter in the flux measurments about their mean value for the period 1963.0 to 1966.0.

The significant result shown in Fig. 5 is that, between 250 and 450 km altitude, the source function is not constant (as one might expect were the proton source solely due to albedo neutron decay), but decreases with increasing altitude according to $S(h)_{obs} \propto h_{min}^{-2.4}$. Also given in Fig. 5 are the altitude dependences of N (at 60 MeV) $\propto h_{min}^{4.7}$ (observed) and $\rho \propto h^{-7.0}$ (computed). As noted by Cornwall et al.,[14] the quantity $S/N\rho$ is a constant under equilibrium conditions. Our results are in good agreement with this condition. The numerical values of S and N in Fig. 5 need be relative only, because it is the ratio S/N that is important here. However, to be somewhat realistic, we have adopted for N (at 60 MeV) at 1963.0 the proton density obtained from the Injun 3 data for $h_{min} = 350$ km, L = 1.40 earth radii.

In their examination of the changes in B-L space with time, Lindstrom and Heckman[15] pointed out that the minimum mirror-point altitudes in the South Atlantic anomaly are decreasing at a rate of $\dot{h} \approx 7$ km/year owing to the secular change of the earth's magnetic field. Such a drift in the minimum mirror-point trajectories in the anomaly produces an apparent source of protons of the amount $S_B = \dot{h}\,(dN/dh)$, where $\dot{h}$ is the inward drift velocity and dN/dh is the altitude gradient of the proton flux. This apparent source is also shown in Fig. 5. We note that its magnitude does not significantly contribute as a proton source at the lower altitudes, comprising only about 2% of S_{obs} at 250 km. However, because of its strong dependence on altitude--e.g., S_B varies as $h^{3.7}$--the S_B source becomes quite significant for higher altitudes, and can account for nearly one half of S_{obs} for altitudes

above 450 km. We wish to stress that the apparent source S_B arises solely from the dynamic behavior of the geomagnetic field, and is independent of any assumptions as to nonadiabatic behavior in the particle motion.

The results of our computations on the solar-cycle variations in the flux of 60-MeV protons are given in Figs. 6 and 7. Figure 6 shows the temporal behavior at 250, 350, and 450 km at L = 1.40 between January 1963 and May 1969. Plotted versus time are the computed ratios j(t)/j(1963.0). The experimental data (Fig. 4) are superimposed on the computed curves for comparison.

The good agreement between the solutions of the continuity equation and our experimental data is most encouraging. Between 1963.0 and 1966.0, the empirical source function S_{obs} reproduces well the observed constancy of the proton flux. As solar activity developed after 1966, the computations show the characteristic differences in the behavior of 60-MeV protons as the altitude--and, hence, lifetimes--increase. Since mid-1967, the calculations indicate that the proton flux at 250 km has sustained a nearly constant minimum value, coincident with the plateau in activity during solar maximum. This is in contrast to the fluxes at 350 and 450 km, which are still decreasing as of early 1969. Such an effect accounts for the apparently high values of J/J_c observed in our last two flights ($\bar{h}_{min}$ = 224 and 299 km).

Starfish Redistribution

Filz and Holeman[10] have reported that an abrupt increase in the low-altitude proton flux followed the Starfish nuclear detonation

on July 9, 1962. At 350 ± 50 km, their data indicate the proton flux was increased by about 7 times over its prebomb level by this event, owing to a nonadiabatic redistribution of the low-altitude protons. On the basis of Filz and Holeman's Fig. 10, we would conclude that the proton flux decayed within 1 year to a constant level, which was some 2.5 times the prebomb level. It is evident, therefore, that the temporal behavior of the inner belt we have been studying has likewise been artificially perturbed. To examine this further, we have carried out the integration of Eq. 1 for the flux $j(t)_{60\ MeV}$ at h_{min} = 350 km beginning 1953.0, under the assumption S_{obs} is time independent. Two initial arbitrary flux values were assumed: (a) $j(1953.0) = 9.2\ cm^{-2}\ sec^{-1}\ MeV^{-1}$, equal to the 60-MeV flux observed in 1964, one full solar cycle later, and (b) $j(1953.0) = 3.2\ cm^{-2}\ sec^{-1}\ MeV^{-1}$. The results of this computation are presented in Fig. 7. Solutions (a) and (b) converge to a unique solution after 1958.5, yielding a $j(t)$ that is independent of initial conditions. Well illustrated is the anticorrelation of the proton flux with the atmospheric density, the latter shown by the dashed line. The computed curves of $j(t)$ from 1958 through 1968 display how flux changes at 60 MeV would have occurred had there been <u>no</u> Starfish detonation and, hence, proton redistribution. Our interpretation of the sequence of events portrayed in Fig. 7 is that, on July 9, 1962, the Starfish detonation caused a rapid increase in the proton flux, and, after an apparently short-lived transient, settled down to a 3-year, steady-state condition. This "steady-state" phenomenon was fortuitously produced when the natural solar-cycle increase in the proton flux was just compensated by the decay of

the Starfish perturbation. The difference between the Starfish and no-Starfish calculations is, in fact, an exponential decay curve. The particle data denoted by circles are form Filz and Holeman;[10] the data of this experiment are shown as X's. All the data are restricted to $\bar{h}_{min} = 350 \pm 50$ km. The two sets of data points are independently normalized to the computed, steady-state condition 1963.0 to 1966.0. We believe it is significant that the relative changes in the (57-MeV) proton flux observed by Filz and Holeman at 350 km altitude, before and after the Starfish detonation, are in agreement with calculations that were, in turn, based on our independently measured post-Starfish data. Finally, we note that the effects of Starfish have now virtually disappeared for altitudes 350 km (and less). Henceforth, the inner-proton belt will be (one hopes) in its "natural" state at these low altitudes.

Semiannual Variations

Recent satellite atmospheric-drag results have revealed that during the course of our particle measurements, the semiannual and solar-cycle density variations in the atmosphere have been comparable in magnitude at altitudes between 191 and 1030 km.[16-19] The semiannual variation has yet to be explained, although the effect has been well documented. Adequate for our purposes here is that, to the extent it has been studied over an 8-year period, the semiannual effect is a highly stable, global phenomenon.[20] Irrespective of altitude and local time, the atmosphere exhibits in-phase world-wide density variations, the minima occurring on about January 26 and July 25, and the maxima on April 1 and November 1. Although the periods between

minima and maxima are not equal, the dates on which they occur have been determined to within an accuracy of several days. The min:max density ratios affected by the semi-variation are typically 1:2. The observed amplitudes of the density variations appear to be related to temperature variations in the thermosphere, the latter being correlated with the intensity of the 10.7-cm solar flux.

It is quite obvious, then, that when proton lifetimes are less than about 6 months, observable semiannual changes in the flux of inner-belt protons should occur. To investigate this statement quantitatively, we have attempted to include in our atmosphere model a realistic description of the semiannual density variations. To do so, we have referred to the works of King-Hele et al. and Cook et al., who have since 1964 examined the semiannual variations at altitudes 191,[16] 470,[17] 480,[18] and 1130 km.[19] We have collected these data and presented them in Fig. 8. To reveal the semiannual variation, diurnal and solar-activity effects have been removed from the data. The residual semiannual variations were then reduced to an $\bar{F}_{10.7}$ that was characteristic of the time during which the atmospheric density measurements were made. The dashed lines through the data are the analytical functions we use to represent the semiannual effect.

We now have a description of a (bounce and drift averaged) Harris and Priester atmospheric model that includes both solar-cycle and empirical semiannual time variations. The flux changes for 60-MeV protons predicted by the continuity equation with this model atmosphere are shown in Fig. 9. Upon comparing this figure with Fig. 6, we see that the semiannual density changes are clearly present at

250 km, but not so at 350 and 450 km Some salient features of these computations that are in accord with the experimental data are:

(a) Between 1963.0 and 1966.0, the semiannual changes in the proton fluxes are small, typically equal to, or less than, the experimental errors. The computed results continue to exhibit a very stable flux level during solar minimum.

(b) As solar activity increases, the average density of the atmosphere increases and the proton lifetimes decrease. Consequently, the response of the trapped protons to changes in the atmosphere becomes more pronounced. This is exemplified by the increasing semiannual oscillations in the proton flux since 1967. The observed amplitudes of the fluctuations in the proton flux measurements since 1967 are consistent with this interpretation.

Because of the preliminary and sensitive nature of the calculations to our atmospheric and magnetic field models, we do not attribute any significance to the fact that the variations in the 350 ± 50-km data appear to be characteristic of an altitude slightly less than 350 km.

Thus far, we have discussed a number of instances in which the experimental data are accounted for by theory. Contrary to this an interesting, and perhaps quite important, observation can be made by closely examining Fig. 9. It is that the observed flux changes are <u>not in phase</u> with the computed semiannual flux variations. Taken at face value, the flux changes appear to be out of phase with the solutions of the continuity equation by about 5 weeks. Surprisingly, this phase difference is such that the proton flux variations are nearly in phase with the semiannual density changes in the atmosphere. The

significance of this observation is certainly not clear at this time. We wish, however, to make the following observation: The principal unknown in the theory of the energetic, inner-belt protons is the source. We have treated the source $S(E, h)$, therefore, as an empirical quantity to be determined by experiment. Using this approach, we find that this empirical source, S_{obs}, decreases with increasing altitude. The only other physical entity that decreases with altitude is the density of the atmosphere. The implication, then, is that there is an effective source of trapped protons related somehow to the atmosphere--indicative of pitch-angle scattering.

SUMMARY

On the basis of our experimental studies on the temporal behavior of low-altitude, inner-belt protons, and their interpretation in terms of solutions of the time-dependent continuity equation, using an empirically determined source function, we make the following conclusions:

(a) The observed temporal changes in the flux of 63-MeV protons since 1963, $220 < \overline{h}_{min} < 450$ km, are in agreement with those expected from the solar-cycle changes in the atmosphere.

(b) The computed time history of the proton flux at 60 MeV before and after the Starfish detonation is in excellent agreement with the observations of Filz and Holeman, as well as with our post-Starfish data.

(c) For altitudes about 250 km, semiannual density changes in the atmosphere should be observable in flux changes of protons $E \lesssim 60$ MeV. That a phase difference may exist between the observed and computed

semiannual changes in the proton flux is unexpected and needs to be explained.

Pitch angle diffusion, which may be an effective source strongly correlated with the atmospheric density, must now be included in the theory in order to see whether or not it can account for the altitude dependence of the source function implicated by our experimental observations.

ACKNOWLEDGMENT

This work was done under the auspices of the U. S. Atomic Energy Commission, the National Aeronautics and Space Administration, Contract NAS 9-5249, and the Lockheed Missiles and Space Company, Independent Research.

REFERENCES

1. H. H. Heckman and G. H. Nakano, J. Geophys. Res. 74, 3575 (1969).
2. G. H. Nakano and H. H. Heckman, Phys. Rev. Letters 20, 806 (1968).
3. S. F. Singer, Phys. Rev. Letters 1, 181 (1958).
4. R. C. Blanchard and W. N. Hess, J. Geophys. Res. 69, 3927 (1964).
5. A. J. Dragt, Solar-cycle Modulation of the Radiation Belt Proton Flux, University of Maryland Technical Report 938, Feb. 1969.
6. J. Valerio, J. Geophys. Res. 69, 4949 (1964).
7. D. C. Jensen and J. C. Cain, J. Geophys. Res. 67, 3568 (1962).
8. H. H. Heckman and A. H. Armstrong, J. Geophys. Res. 67, 1255 (1962).
9. S. C. Freden and R. S. White, J. Geophys. Res. 65, 1377 (1960).
10. R. Filz and E. Holeman, J. Geophys. Res. 70, 5807 (1965).
11. H. H. Heckman and V. Brady, J. Geophys. Res. 71, 2791 (1966).
12. I. Harris and W. Priester, J. Geophys. Res. 67, 4585 (1962); also NASA Tech Note No. D-1444 (1962).
13. I. Harris and W. Priester, J. Geophys. Res. 68, 5891 (1963).
14. J. M. Cornwall, A. R. Sims, and R. S. White, J. Geophys. Res. 70, 3099 (1965).
15. P. J. Lindstrom and H. H. Heckman, J. Geophys. Res. 73, 3441 (1968).

16. D. G. King-Hele and J. Hingston, Planetary Space Sci. 16, 675 (1968).

17. D. G. King-Hele and D. M. C. Walker, Planetary Space Sci. 17, 197 (1969).

18. D. G. King-Hele and J. Hingston, Planetary Space Sci. 16, 937 (1968).

19. G. E. Cook and D. W. Scott, Planetary Space Sci. 15, 1933 (1967).

20. L. G. Jacchia, J. W. Slowey, and I. G. Campbell, Planetary Space Sci. 17, 49 (1969).

FIGURE CAPTIONS

Fig. 1. The South Atlantic anomaly. The heavy-line contours are Injun 3 isoflux contours for protons $40 < E < 110$ MeV at 400 km altitude. Dashed lines are contours of L using the Jensen and Cain 48-coefficient field model. The northward traversals of a satellite, 75° orbit inclination, during a 4-day flight are shown as arrows.

Fig. 2. Omnidirectional flux of 63-MeV protons versus average minimum-mirror-point altitude during solar minimum, November 1962–June 1966. Experimental data are shown as open circles; the least-square fit to these data is denoted by J_c. Computed Injun 3 daily fluxes and least-squares fit are shown by the solid points and dashed line.

Fig. 3. Differential energy spectrum for protons, $E > 57$ MeV, 1963-1966. Dashed curve is a smoothed fit to the spectrum measured in 1960 by Heckman and Armstrong (Ref. 8).

Fig. 4. Temporal behavior of the 63-MeV omnidirectional proton flux, September 1962 to May 1969. Plotted are the ratios $J(t)/J_c$ versus time, where J_c is the least-squares fit to the data for the period November 1962 to June 1966.

Fig. 5. Altitude dependence of source function of 60-MeV protons, S_{obs}, required to account for a constant flux level observed between 1963.0 and 1966.0. The altitude dependence of the measured proton density, N(h), and computed effective atmospheric density, $\rho(h)$, for 1963.0 are also shown. The source S_B is the

apparent source of 60-MeV protons arising from the lowering of the mirror-point trajectories owing to the secular variation of the geomagnetic field.

Fig. 6. Computed ratios of j(t)/j(1963.0) at 60 MeV at minimum-mirror point altitudes 250, 350, and 450 km, L = 1.40, between January 1963 and May 1969, given source S_{obs}. Flux data from Fig. 4 are also shown.

Fig. 7. Computed proton flux $j(t)_{60\ MeV}$ at h_{min} = 350 km, beginning 1953.0, assuming source S_{obs} is constant, and initial flux values j(1953) = 9.2 and 3.2 $cm^{-2}\ sec^{-1}\ MeV^{-1}$. Unique solution is obtained at this altitude after 1958.5. The Starfish redistribution on July 9, 1962, the 3-year "steady-state," 1963-1966, and the abrupt solar-cycle decrease in the proton flux after mid-1966 are reproduced in these calculations. The data denoted by open circles are from Ref. 10; the x's, this experiment. The data points are limited to $\bar{h}_{min} = 350 \pm 50$ km. Solar-cycle behavior of atmosphere at 350 km altitude is given by the dashed curve.

Fig. 8. Semiannual density variations in the atmosphere, reproduced from Refs. 16-19. Dashed curves are analytic functions used to represent the semiannual density changes in the computations.

Fig. 9. Calculated j(t)/j(1963.0) at 60 MeV at h_{min} = 250, 350, and 450 km when both solar-cycle and semiannual density changes are incorporated into the continuity equation. Again, the experimental data are shown for comparison with the theory.

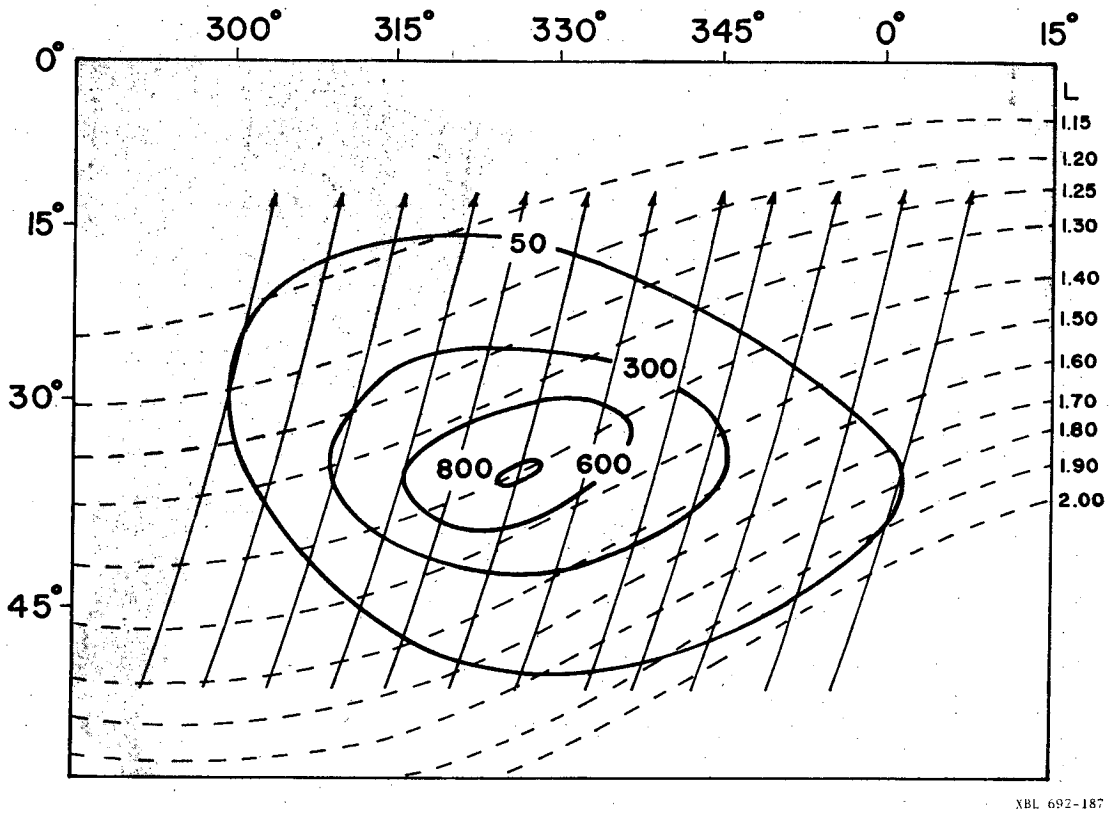
300°
315°
330°
345°
0°
15°
0°
15°
30°
45°
L
1.15
1.20
1.25
1.30
1.40
1.50
1.60
1.70
1.80
1.90
2.00
50
300
600
800
XBL 692-187

Fig. 1

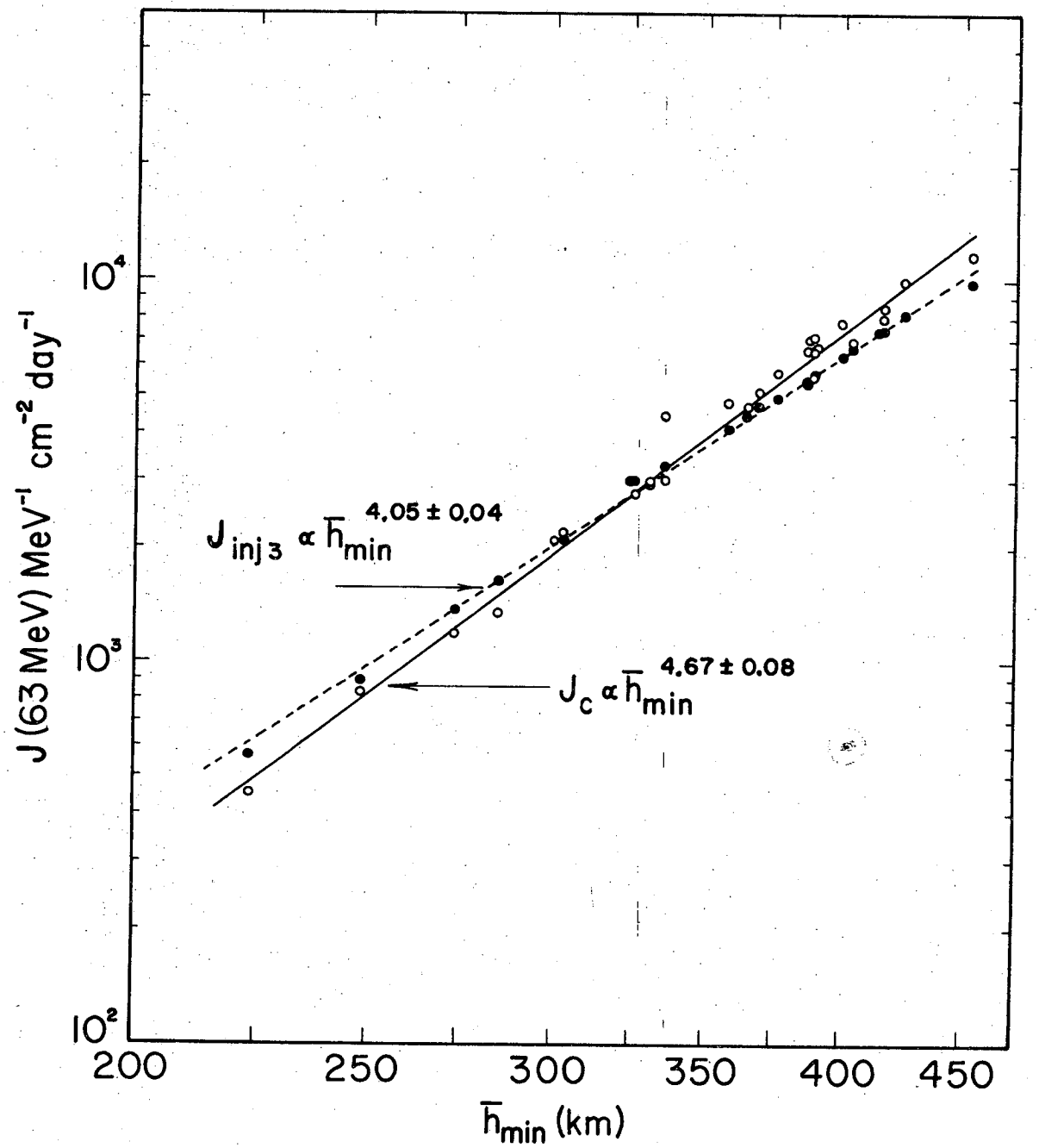

XBL 6810-6113

Fig. 2

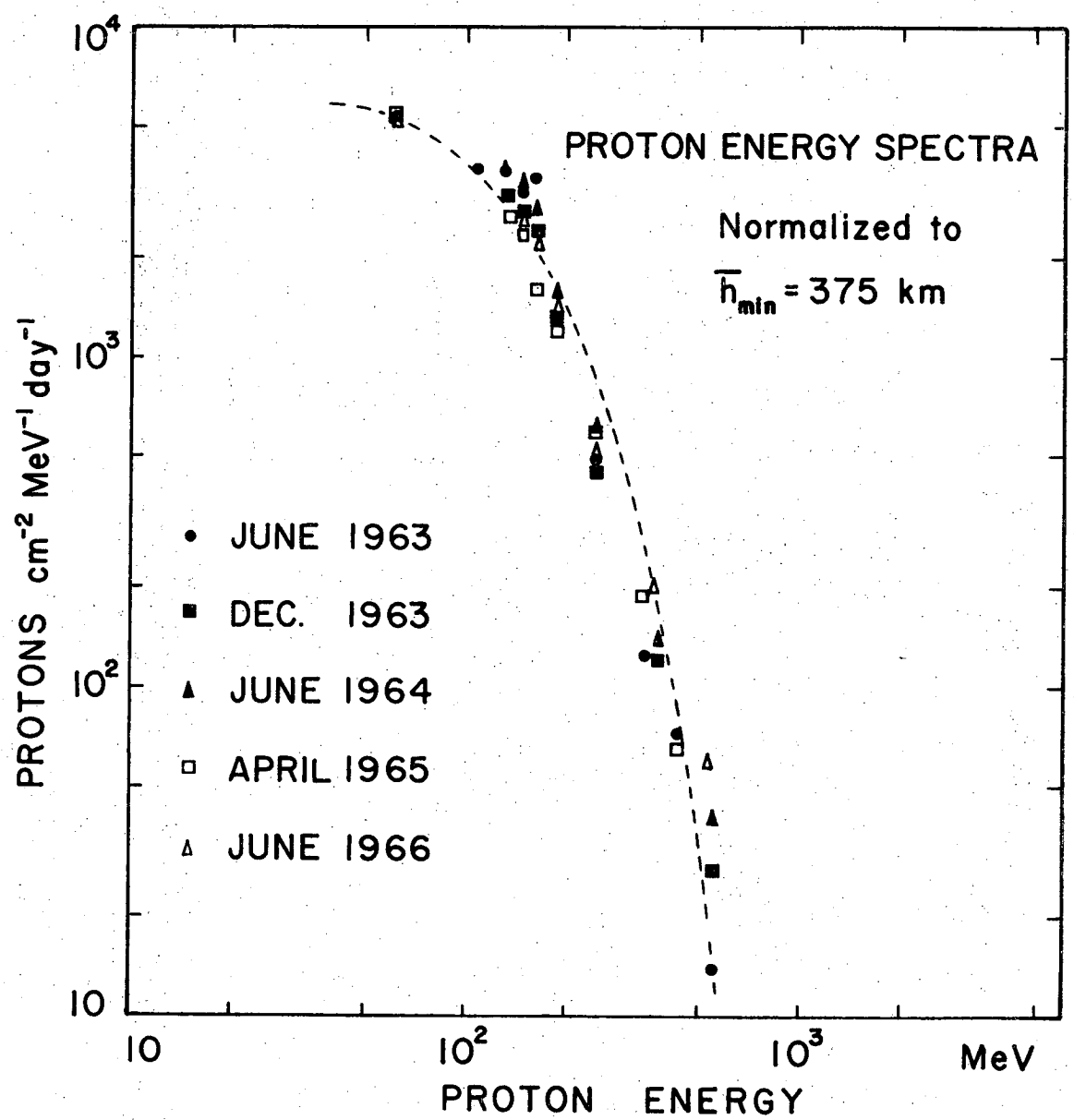

XBL 6810-6114

Fig. 3

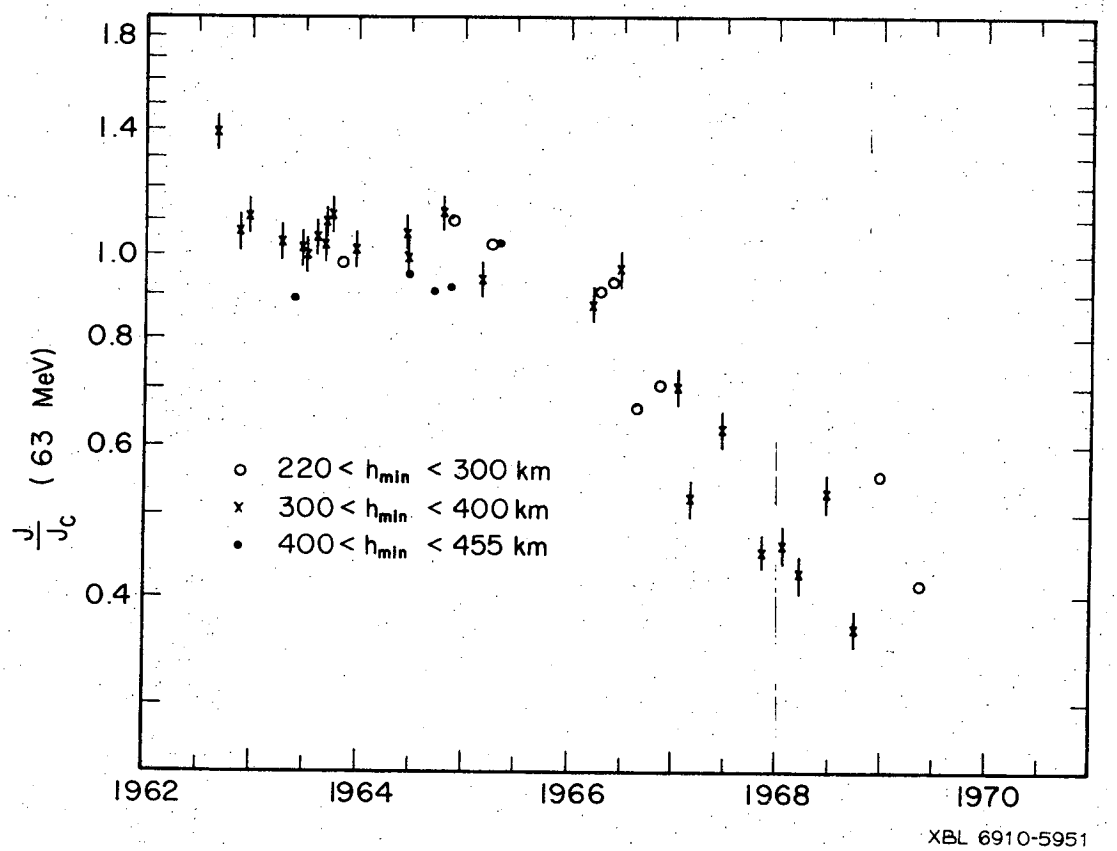
1.8
1.4
1.0
0.8
0.6
0.4
J/Jc (63 MeV)
220 < hmin < 300 km
300 < hmin < 400 km
400 < hmin < 455 km
1962
1964
1966
1968
1970
XBL 6910-5951

Fig. 4

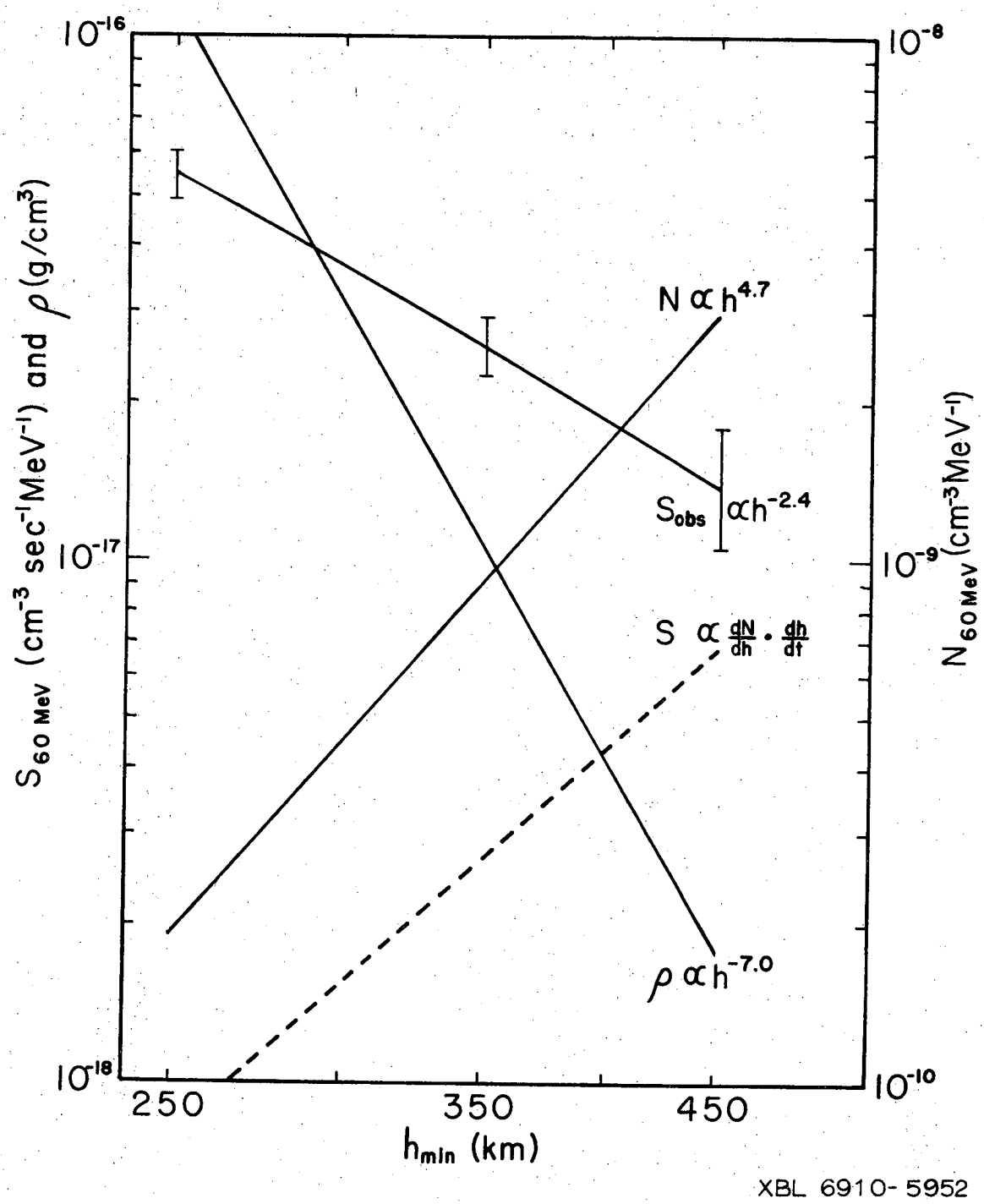
10^{-16}
10^{-17}
10^{-18}
10^{-8}
10^{-9}
10^{-10}
$S_{60\,MeV}$ (cm^{-3} $sec^{-1}MeV^{-1}$) and ρ (g/cm^3)
$N_{60\,MeV}$ ($cm^{-3}MeV^{-1}$)
$N \propto h^{4.7}$
$S_{obs} \propto h^{-2.4}$
$S \propto \frac{dN}{dh} \cdot \frac{dh}{dt}$
$\rho \propto h^{-7.0}$
250
350
450
h_{min} (km)
XBL 6910-5952

Fig. 5

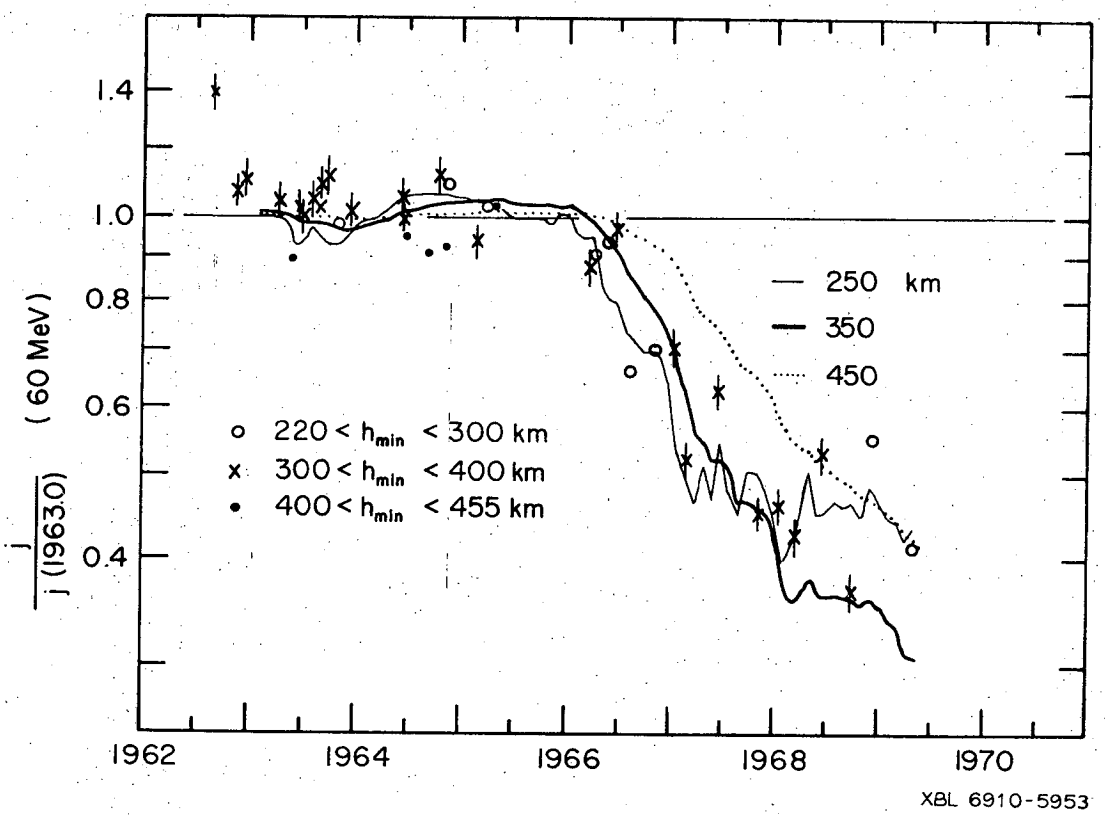
1.4
1.0
0.8
0.6
0.4
j / j (1963.0) (60 MeV)
1962
1964
1966
1968
1970
250 km
350
450
220 < h_min < 300 km
300 < h_min < 400 km
400 < h_min < 455 km
XBL 6910-5953

Fig. 6

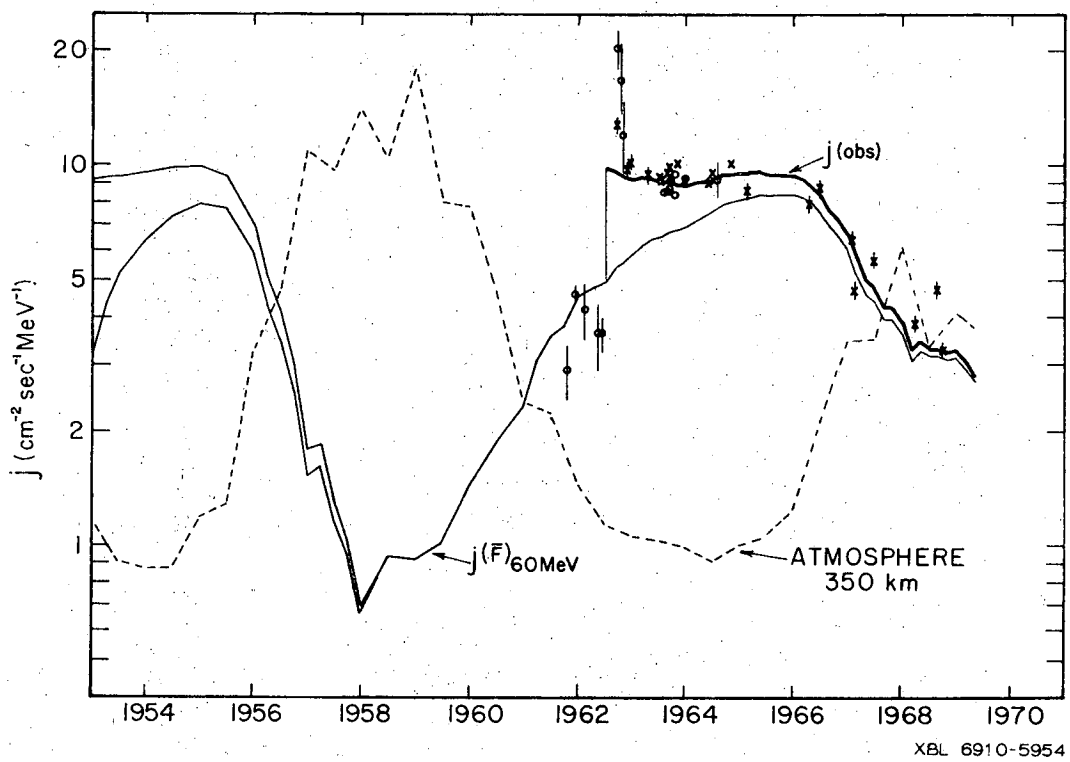
20
10
5
2
1
j (cm⁻² sec⁻¹ MeV⁻¹)
j (obs)
j(F)60MeV
ATMOSPHERE
350 km
1954
1956
1958
1960
1962
1964
1966
1968
1970
XBL 6910-5954

Fig. 7

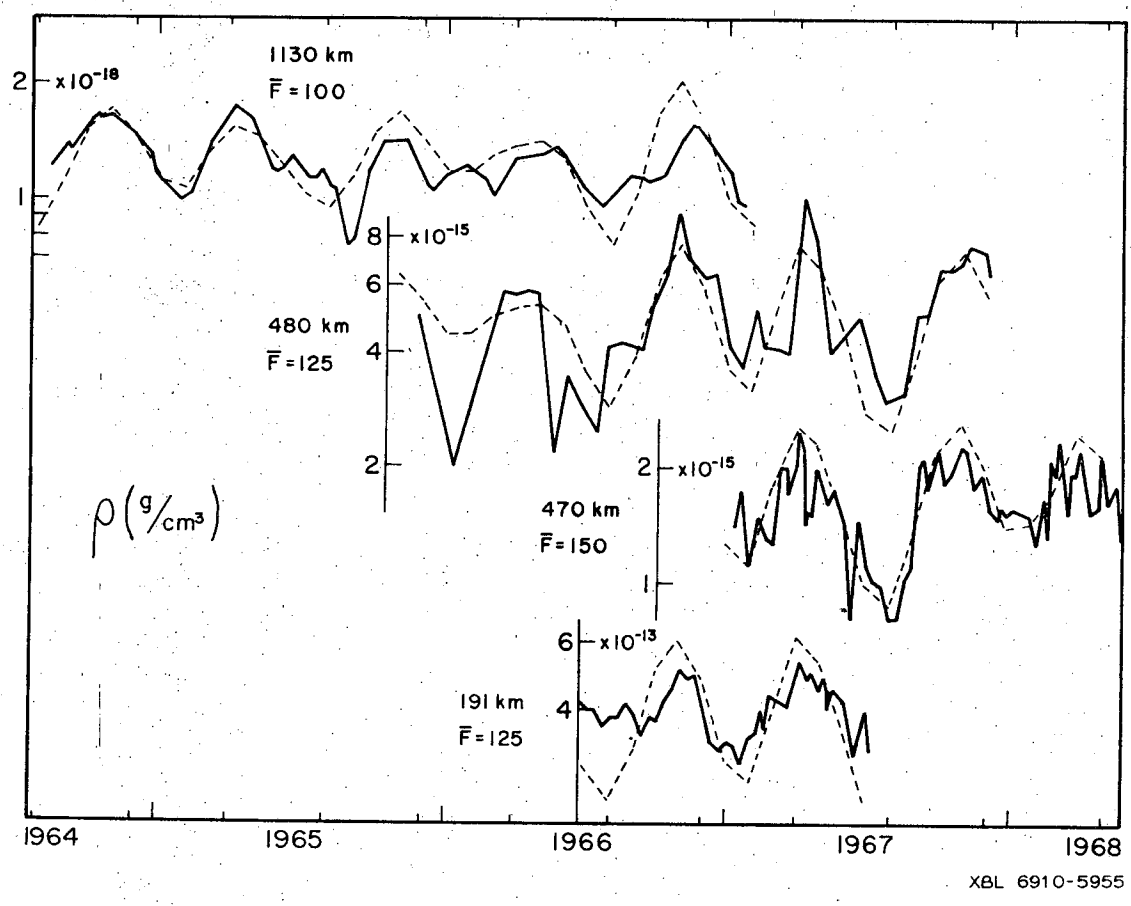
1130 km
F̄ = 100
x10⁻¹⁸
2
1
480 km
F̄ = 125
x10⁻¹⁵
8
6
4
2
470 km
F̄ = 150
x10⁻¹⁵
2
1
191 km
F̄ = 125
x10⁻¹³
6
4
ρ (g/cm³)
1964
1965
1966
1967
1968
XBL 6910-5955

Fig. 8

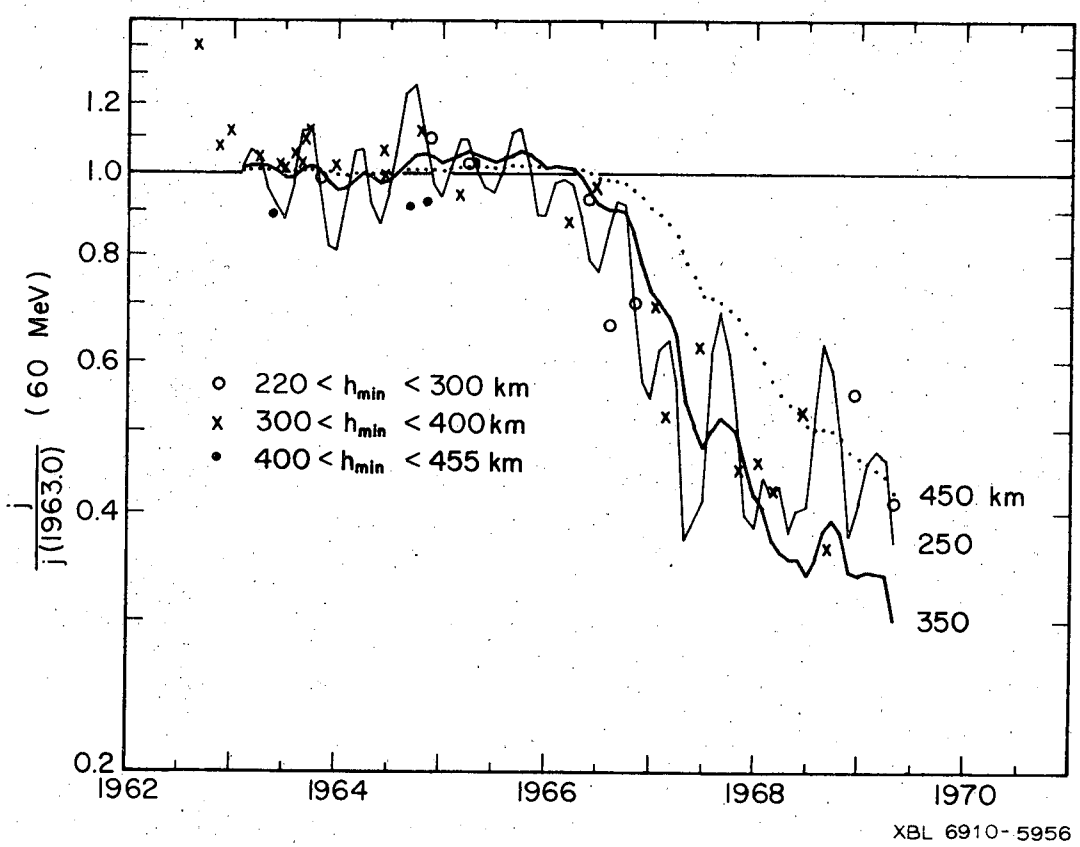
1.2
1.0
0.8
0.6
0.4
0.2
1962
1964
1966
1968
1970
j / j(1963.0) (60 MeV)
220 < h_min < 300 km
300 < h_min < 400 km
400 < h_min < 455 km
450 km
250
350
XBL 6910-5956

Fig. 9

LEGAL NOTICE

This report was prepared as an account of Government sponsored work. Neither the United States, nor the Commission, nor any person acting on behalf of the Commission:

A. Makes any warranty or representation, expressed or implied, with respect to the accuracy, completeness, or usefulness of the information contained in this report, or that the use of any information, apparatus, method, or process disclosed in this report may not infringe privately owned rights; or

B. Assumes any liabilities with respect to the use of, or for damages resulting from the use of any information, apparatus, method, or process disclosed in this report.

As used in the above, "person acting on behalf of the Commission" includes any employee or contractor of the Commission, or employee of such contractor, to the extent that such employee or contractor of the Commission, or employee of such contractor prepares, disseminates, or provides access to, any information pursuant to his employment or contract with the Commission, or his employment with such contractor.

TECHNICAL INFORMATION DIVISION
LAWRENCE RADIATION LABORATORY
UNIVERSITY OF CALIFORNIA
BERKELEY, CALIFORNIA 94720